Original Article

A Magnetically Recoverable and Highly Effectual Fe_3O_4 Encapsulated MWCNTs Nano-Composite for Synthesis of 1,8-Dioxo-octahydroxanthene Derivatives

Mantosh B. Swami[a] | Ganpat R. Nagargoje[b] | Sushil R. Mathapati[c] | Abhay S. Bondge[d] | Arvind H. Jadhav[e] | Sharad P. Panchgalle[f] | Vijaykumar S. More[g,*]

[a]*Department of Chemistry, Mahatma Basweshwar Mahavidyalay, Latur, 413512, India*
[b]*Deptartment of Chemistry, Shivaji Mahavidyalaya, Renapur, Dist-Latur-413527, India*
[c]*Department of Chemistry, Shri Madhavrao Patil Mahavidyalaya, Murum, 413605, India*
[d]*Department of Chemistry, Shivneri Mahavidyalaya, Shirur Anantpal Dist-Latur-41354, India*
[e]*Centre for Nano and Material Sciences, Jain University, Bangalore-562112, India*
[f]*Department of Chemistry, K. M. C. College, Khopoli, Dist-Raigad- 410203, India*
[g]*Department of Chemistry, Kai. Rasika Mahavidyalaya Deoni, Dist-Latur-413519, India*

Use your device to scan and read the article online

Citation M.B. Swami, G.R. Nagargoje, S.R. Mathapati, A.S. Bondge, A.H. Jadhav, S.P. Panchgalle, V.S. More. **A Magnetically Recoverable and Highly Effectual Fe_3O_4 Encapsulated MWCNTs Nano-Composite for Synthesis of 1,8-Dioxo-octahydroxanthene Derivatives.** *J. Appl. Organomet. Chem.*, **2023**, *3*(3), 184-198.

https://doi.org/10.22034/JAOC.2023.404091.1085

Article info:
Received: 25 June 2023
Accepted: 26 July 2023
Available Online: 01 August 2023
ID: JAOC-2306-1085
Checked for Plagiarism: Yes
Language Editor checked: Yes

Keywords:
Magnetically recovered, Heterogeneous and recyclable catalyst, 5, 5-Dimethyl 1, 3-cyclohexanedione, 1, 8-Dioxooctahydroxanthene derivatives

ABSTRACT

1,8-Dioxooctahydroxanthene derivatives were synthesized from 5,5-dimethyl-1,3-cyclohexanedione and substituted aromatic aldehydes in attendance of Fe_3O_4@OMWCNT aseco-friendly and recyclable nano-catalyst. The heterogeneous and magnetically separable catalyst was prepared as per procedure and characterized with help of analytical tools. After successful characterization of catalyst, it was used for present transformation, which reported 90-96% yield of isolated product. Key advantages of this method are magnetically separable and reusable catalyst, improved yield, short time, less expensive, and easy handling of reaction procedure.

Introduction

In multicomponent reactions, more than two substrates react to give a product, it involves all essential atoms from reactant. These are more convenient and useful compared to traditional method of stepwise synthesis of target molecule. In multicomponent reactions, target molecule is synthesized by adding number of reactants in one pot and single step. MCRs were performed via simple experimental procedure without need of any special conditions [1]. These types of reactions have been studied widely in organic synthesis, because of generation of new functionality in target molecule from simple

***Corresponding Authors: Vijaykumar S. More** (vijaymore@gmail.com)

starting material in one-pot reactions [2]. The importance of this method is due to considerably reduction of efforts and time.

Among the various MCRs, synthesis of xanthene is one of the methods, which paying attention of larger audience from researcher and academic community due to the importance of xanthene in several fields. However, xanthene derivative possesses various applications in biological and pharmaceutical field. Derivatives of xanthenes are reported as anti-inflammatory [3], antibacterial [4], antiviral [5], anti-tumor [6], anti-proliferative [7, 8], anticancer [9, 10], anti-oxidant [11], and antiplasmodial [12], also acts as trypanothione reductase inhibitor [13] and selective estrogen receptor modulator [14]. In addition, these compounds were used as fluorescent materials in biological process [15], luminescent sensors [16], xanthene-fluorescence based probes for optical imaging applications [17]. Even though, these are used in blocking of zoxazolamine induced paralysis [18], some derivatives of xanthene like xanthenediones are versatile synthons in organic synthesis chemistry owing to presence of reactive structural unit. Nowadays, considerable interest of researchers has been enhanced in synthesis of fused heterocycles, due to its plenty of applications in the field of biological and material science.

Literature includes number of methods for the synthesis of the xanthenes, these includes cycloaddition of cyclic aryltriflate esters [19], cyclization of 2-hydroxy aryl aldehyde and 2-tetralone [20], cyclization of benzynes with phenols [21], via Grignard reagent and triethyl orthoformate [22], etc. Conversely, synthesis of 1, 8-dioxooctahydroxanthenes has been worked out using a variety of catalysts and solvent systems.

Amid such various protocols, the well-established technique for synthesis of 1, 8-dioxooctahydroxanthenes encompasses cyclization between dimedone and various substituted benzaldehyde in presence of different catalysts. However, lot of methods suffers from some drawbacks, such as longer time, hazardous and expensive solvent, harsh reaction conditions, expensive chemicals, tedious work up, recovery of catalyst, and poor yield. Therefore, there was a scope to develop proficient technique for one-pot synthesis of 1, 8-dioxo- octahydroxanthene derivatives.

From the last decade, multi walled carbon nanotubes (MWCNTs) have been used as prominent support material for homogeneous reactions. The pure MWCNT based materials provides high dispersion of catalyst, which significantly increases the surface between the active catalytic sites and reactants [23]. Recently, great attention has been received for functionalization of MWCNT with number of inorganic materials for improving their properties and applications in diverse fields [24-25]. Subsequently, the successful conversion of multi walled carbon nanotube to MWCNT-Fe_3O_4 composite is one of the great demand due to its significant use in different field such as catalysis, storage of magnetic data, electronic tools, electrochemical biosensing, imaging, toners, as adsorbent, magnetically governed drug delivery system, nanoprobes, and biomedicine [26-29]. Due to such attractions of surface modified MWCNTs with Fe_3O_4, we intended to prepare it and screened for xanthene synthesis.

In present protocol, we have reported efficient conversion of dimedone and substituted benzaldehyde to 1, 8-dioxooctahydroxanthenes in presence of catalytic amount of freshly prepared MWCNT-Fe_3O_4. The reaction parameters were finalised after the optimization. We also investigated the reusability of MWCNTs-Fe_3O_4 nano-catalyst and deliberated its role in present transformation through probable mechanism.

Experimental

Instruments and reagents

Multi-walled carbon nanotubes, potassium permanganate and sulphuric acid (98 %), other reagents, solvents were obtained from Sigma Aldrich and checked their purity before use. Distilled water and methanol were used in the reaction for synthesis and purification of the MWCNTs-Fe_3O_4 catalyst.

Catalyst preparation

Oxidation of MWCNTs

Carboxylic group were imparted by oxidation of MWCNTs, these modification of MWCNTs was done as per literature [15, 25]. 6.0 g of MWCNTs was added to the solution of 140 ml of sulphuric acid and nitric acid (3:1) in a 1000 mL round bottom flask. The obtained reaction mixture was ultrasonicated for 4 h at room temperature, and then it was cooled up to 0 °C. After that, sonicated mixture was reacted with 18 g of potassium permanganate (KMnO4) under temperature below 15 °C, and then the reaction mixture was stirred for one and half-hour under maintained temperature. There after, it was diluted with adding 300 mL of distilled water and heated up to 90 °C with continues stirring for 30 minutes. Further more, 850 mL of water was added in the reaction composition and filtered using PVDF filter papers with the help of a vacuum pump. The oxidised MWCNTs (COOH-MWCNTs) were washed using distilled water and dried at 60 °C for overnight, under vacuum.

Synthesis of Fe_3O_4-oxidized MWCNTs (Fe_3O_4@OMWCNTs)

Fe_3O_4-oxidized MWCNTs catalyst was prepared using chemical co-precipitation method. The oxidised MWCNTs (90 mg) was reacted with aqueous solution (25 ml) of 0.4 mmol (157 mg) $(NH_4)_2Fe(SO_4)_2 \bullet 6H_2O$ and 0.8 mmol (386 mg) $NH_4Fe(SO_4)_2 \bullet 12H_2O$ at 50 °C, and then the mixture was sonicated for 10-15 minutes and aqueous solution of ammonium hydroxide (5 ml) was added which produces precipitation of iron oxide. The stirring of reaction mixture was continued at 50 °C for half an hour. Finally, the obtained solid was separated from the reaction container using external strong magnet. There after, the separated magnetically active material was purified followed by number of washing with distilled water and dried in oven at 120 °C for 24 hours.

General procedure for synthesis of 1,8-dioxooctahydroxanthene using Fe_3O_4@OMWCNTs catalyst

A 100 ml RB flask charged with substituted aldehyde (1 mmol), 5, 5-dimethyl-1, 3-cyclohexanedione (2 mmol), and Fe_3O_4@OMWCNTs (10 wt %), the resultant mixture was refluxed in 10 ml of ethanol till completion of reaction, which was monitored via TLC technique (Hexane:EA; 8:2) (**Scheme 1**). After successful transformation of reactants to product, the catalyst was separated using external magnet without filtration and solvent evaporated. The solid of targeted product was filtered off, and then recrystallized in hot ethanol to acquire pure xanthene derivatives. Formation of target molecule was confirmed with spectral analysis and comparative study of analytical data with data existing in literature [30-32].

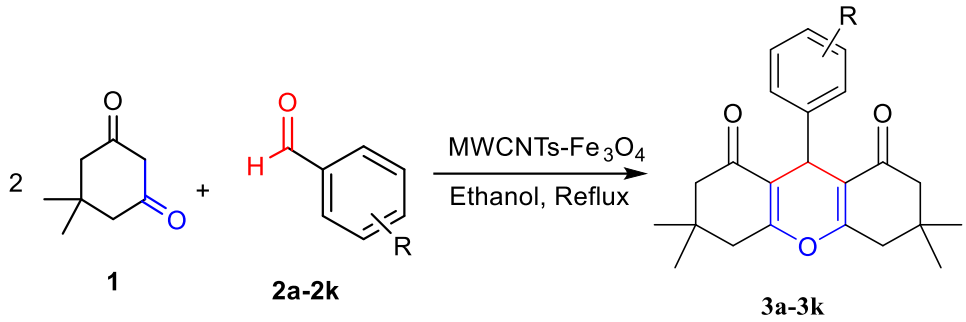

Scheme 1. Synthesis of xanthene derivatives in the presence of prepared Fe_3O_4@OMWCNTs catalyst

Spectral analysis of selective derivatives of xanthenes

*3,3,6,6-tetramethyl-9-(4-methylphenyl)-1,8-dioxooctahydroxanthene (**3a**)*

FT-IR (KBr, in cm^{-1}): 3032, 2960, 2872, 1664, 1622, 1356, 1197, 1165, 1140, 1000, and 844;**^{1}H-NMR** ($CDCl_3$, in δ ppm): 7.15 (d, 2H), 7.03(d, 2H), 4.72 (s, 1H), 2.46 (s, 4H), 2.25 (s, 3H), 2.16 (q, 4H), 1.08(s, 6H), and 0.97 (s, 6H); **^{13}C-NMR** ($CDCl_3$, in δ ppm): 196.2, 162.1, 141.3, 135.8, 128.4, 128.21, 115.8, 50.6, 40.8, 32.3, 31.5, 29.2, 27.4, and 21.2; **MS** (m/z): 365.28 (M^+).

*9-(4-Hydroxyphenyl)-1,8-dioxo-octahydroxanthene (**3c**)*

FT-IR (KBr, in cm^{-1}): 3433, 2952, 1644, 1555, 1376, 1235, 1197, 1188, 776; **^{1}H-NMR** ($CDCl_3$, in δ ppm): 9.16 (s, 1H), 6.92 (d, 2H), 6.57 (d, 2H), 4.45 (s, 1H), 2.48-2.65 (m, 4H), 2.22-2.30 (m, 4H), 1.96-2.12 (m, 2H), and 1.78-1.89 (m, 2H); **^{13}C-NMR** ($CDCl_3$, in δ ppm): 196.83, 164.95, 156.07, 135.50, 129.30, 116.38, 115.11, 36.90, 30.20, 26.87, and 20.34; **MS** (m/z): 367.1(M^+).

*3,3,6,6-Tetramethyl-9-(4methoxy-phenyl)-1,8-dioxooctahydro-xanthene (**3d**)*

FT-IR (KBr, in cm^{-1}): 3058, 2959, 2877, 1664, 1627, 1512, 1463, 1358, 1261, 1194, 1109, 1032, 844, and 564; **^{1}H-NMR** ($CDCl_3$, in δ ppm): 7.22 (d, 2H), 6.77 (d, 2H), 4.68 (s, 1H), 3.74 (s, 3H), 2.45 (s, 4H), 2.19 (q, 4H), 1.08 (s, 6H), 0.99 (s, 6H); **^{13}C-NMR** ($CDCl_3$, in δ ppm): 196.72, 162.00, 157.86, 136.52, 129.42, 115.80, 113.52, 55.22, 50.80, 40.92, 32.30, 30.83, 29.22, and 27.40; **MS** (m/z): 381.20 (M^+).

*3,3,6,6-tetramethyl-9-(4-chloro-phenyl)-1,8-dioxooctahydroxanthene (**3e**)*

FT-IR (KBr, in cm^{-1}): 3032, 2964, 2954, 1677, 1662, 1468, 1362, 1199, 1168, 1004, 852; **^{1}H-NMR**($CDCl_3$, in δ ppm): 7.18 - 7.25 (dd, 4H), 4.72 (s, 1H), 2.18 (q, 4H), 2.46 (s, 4H), 1.12 (s, 6H), and 1.00 (s, 6H); **^{13}C-NMR** ($CDCl_3$, in δ ppm): 191.10, 157.18, 137.44, 126.78, 124.54, 122.98, 110.04, 45.46, 35.62, 26.96, 26.23, 24.04, and 22.06; **MS** (m/z): 385.2 (M + H).

*3,3,6,6-tetramethyl-9-(4-hydroxy-3-methoxy-phenyl)-1,8-dioxooctahydroxanthene (**3f**)*

FT-IR (KBr, in cm^{-1}): 3414, 3025, 2957, 1668, 1625, 1516, 1433, 1358, 1279, 1228, 1198, 1136, 1027, and 625,574; **^{1}H-NMR** ($CDCl_3$, in δ ppm): 7.03 (s, 1H), 6.74 (d, 1H), 6.57 (dd, 1H), 5.48 (bs, 1H), 4.67 (s, 1H), 3.85 (s, 3H), 2.48 (s, 4H), 2.22 (q, 4H), and 1.02 (s, 12H); **^{13}C-NMR** ($CDCl_3$, in δ ppm): 196.5, 162.2, 145.9, 144.2, 136.5, 120.2, 115.8, 113.8, 112.3, 55.4, 50.5, 40.5, 32.4, 31.4, 29.3, and 27.4; **MS** (m/z): 419.40 (M^+).

*3,3,6,6-Tetramethyl-9-(4-nitrophenyl)-1,8-dioxo-octahydroxanthene (**3i**)*

FT-IR (KBr, in cm^{-1}): 3022, 2928, 1686, 1655, 1530, 1368, 1188, 1033, 855, 756, 633, and 513; **^{1}H-NMR**($CDCl_3$, in δ ppm): 8.11 (d, 2H), 7.38 (d, 2H), 4.85 (s, 1H), 2.88 (s, 4H), 2.33 (s, 4H), 1.14 (s, 6H), and 1.01 (s, 6H); **^{13}C-NMR** ($CDCl_3$, in δ ppm): 197.20, 164.82, 148.64, 133.10, 131.42, 128.32, 126.80, 115.72, 114.40, 51.82, 43.90, 43.62, 30.10, 29.51, 27.61, and 27.4; **MS** (m/z): 395 [M^+].

Results and Discussion

Characterization of prepared catalyst

FT-IR analysis

Analysis of functional groups present on surface modified MWCNTs catalyst was determined with help of stretching and bending vibrations in FT-IR spectrum as seen in **Figure 1**. The signal at 3344 cm^{-1} exhibited O-H stretching frequency, which indicated the presence of O-H functionality on the wall of MWCNTs, which specified adsorption of water molecule from atmospheric moisture [33–35]. Correspondingly, two intense bands observed at 2869 cm^{-1} and 3022 cm^{-1} indicated the C-H stretching.

The FT-IR spectrum displayed several signals amid 1390-1640 cm^{-1}, showed presence of aromatic building units in MWCNTs [36,37]. After oxidation process, prominent additional peaks for C=O functionality were observed at 1740 cm^{-1} which clearly indicated creation of COOH group [34-37]. The FT-IR spectrum of Fe_3O_4@OMWCNTs catalyst consists with all exactly similar signals as in OMWCNTs with one

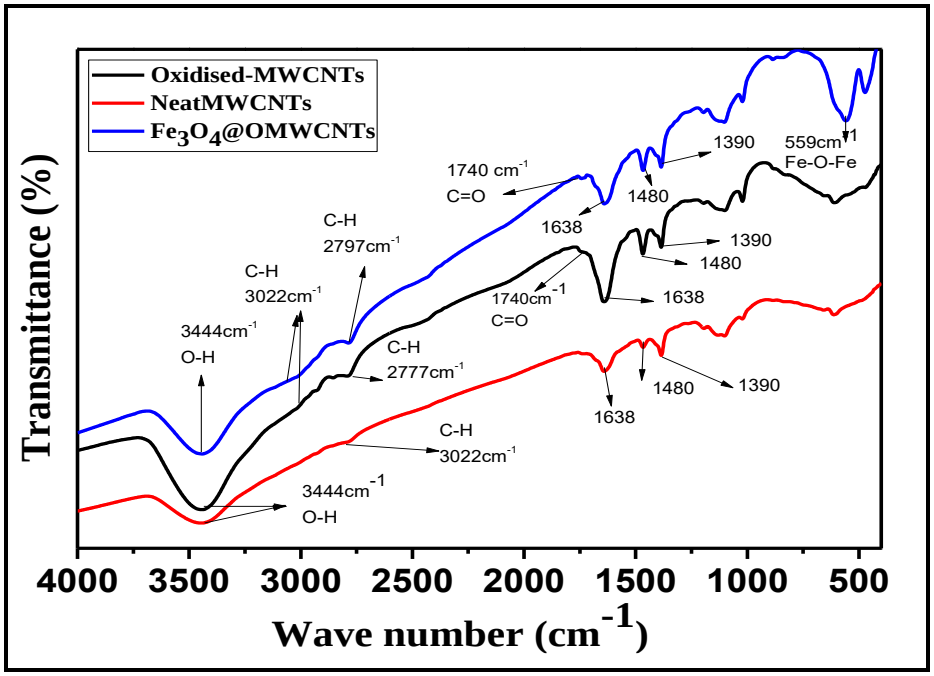

Figure 1. FT-IR spectrum of **a**) MWCNTs, **b**) OMWCNTs, **c**) Fe_3O_4@OMWCNTs

additional peak for Fe-O-Fe stretching at 559 cm^{-1}. The prepared catalyst Fe_3O_4@OMWCNTs displayed Fe-O-Fe stretching peaks along with all signals for OMWCNTs [38]. Form this observation, we have concluded that the successful dispersion of the Fe_3O_4 nanoparticles over the OMWCNTs and formation of OMWCNT-Fe_3O_4 nano-composite. In addition, FT-IR spectrum of Fe_3O_4@OMWCNTs (**Figure 1** (iii)) is free from any additional peaks that indicated the 100% purity of prepared nano-composite.

XRD analysis

The crystalline nature of prepared Fe_3O_4@OMWCNTs catalyst was deliberated through the comparative study of XRD pattern with MWCNTs and OMWCNTs (**Figure 2**). The XRD spectrum of MWCNTs and OMWCNTs displayed distinguishing signals at 002 and 100 plans at 2θ values of 26° and 42°, respectively (JCPDS file no. 33-0664). These results exhibited the crystalline nature of both pure MWCNTs and OMWCNTs, while the intensity of peaks were observed somewhat decreases for OMWCNTs and is due to the modification of MWCNT surface through introduction of oxidized functionality by ruptured surface [39].

Figure 2 (iii) showed XRD pattern of Fe_3O_4@OMWCNT, it exhibited signals for OMWCNT and Fe_3O_4 nanoparticles. XRD of Fe_3O_4@OMWCNT catalyst represented the peaks at 2θ values 18.4° for plane (111), 30.3° for plane (220), 35.7° for plane (311), 37.3° for plane (222), 43.3° for plane (400), 53.8° for plane (422), 57.3° for plane (511), and 62.9° for plane (440) which were exactly similar planes observed in XRD pattern of Fe_3O_4 (JCPDS file 19-0629, Fe_2O_3) [40]. The average particles size of crystallite Fe_3O_4 was near about 20 nm and determined through Debye-Scherrer Equation [41]. Accordingly, we reported as the successful formation nano-crystals of iron oxide dispersed over the OMWCNTs surface.

Surface area determination

The surface area and specific pore volume of prepared material has been calculated using nitrogen adsorption and desorption technique. Likewise, BET technique was used to calculate surface area, pore size and specific active cites of the prepared nano-particles accessible as efficient catalyst for the current

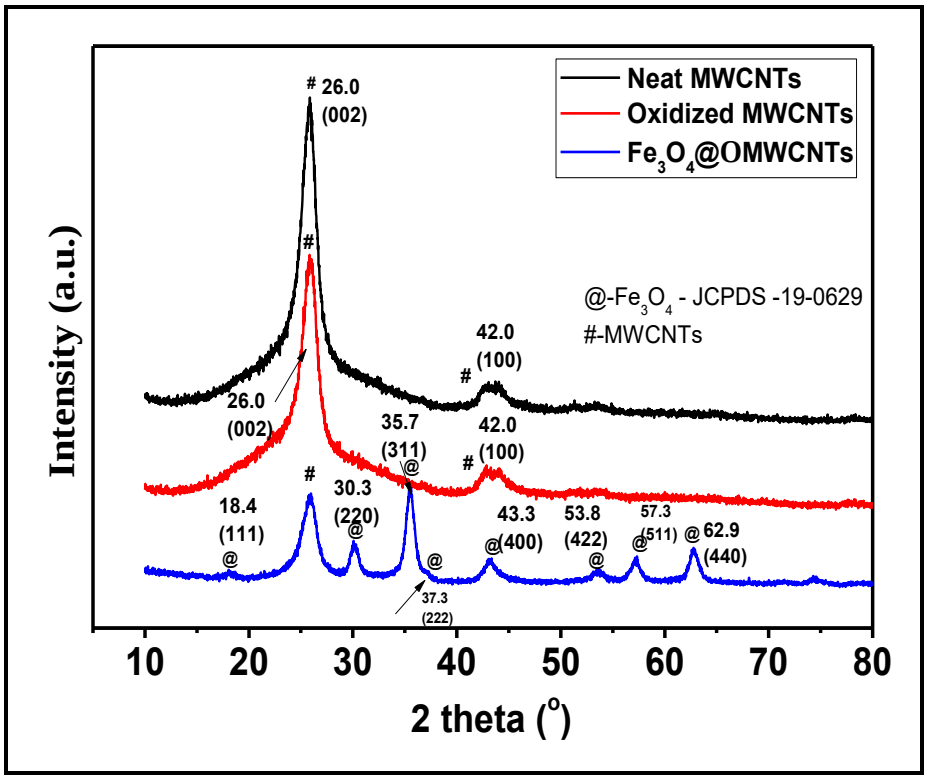

Figure 2. Analysis of XRD pattern (i) MWCNTs, (ii) OMWCNTs, and (iii) Fe_3O_4@OMWCNTs

transformation. The specific surface area of pure MWCNTs was observed as 117.59 m^2g^{-1} and average pore diameter was found to be 3.95 nm. BET study showed that, reduction in the surface area to 113.48 and average pore diameter to 3.57 of oxidised MWCNTs as compared to pure MWCNTs was due to oxidation functionalities covered the surface of MCNTs. Furthermore, according to **Figure 3**, it was clearly indicated that the reduction in total specific surface area up to 86.638 m^2g^{-1} while average pore diameter of Fe_3O_4@OMWCNTs nano-crystals were found to be 3.48 nm. From these outcomes, it was confirm that the scattering of Fe_3O_4 over the OMWCNTs surface that resulted in reduction of surface area and average diameter of pore. Besides, we have studied comparative colour of pure MWCNTs and prepared catalyst. As seen, MWCNT has black colour, highly smooth powder, while after oxidation, it turned in greyish black colour, it supplementary support to successfully oxidation of MWCNT. Correspondingly, adsorption of Fe_3O_4 nanoparticles on the OMWCNT surface turns greyish black powder to reddish brown colour powder of expected catalyst. These results are well coincided with the data available in literature [41, 42].

Thermo gravimetric analysis of catalyst

Figure 4 showed comparative TGA analysis of MWCNTs, OMWCNTs, and Fe_3O_4@OMWCNTs. Initially, we have inspected the neat MWCNT sample for TGA study. It was found that the 42% weight loss in MWCNT at 550 °C and onwards remain stable up to 1000 °C, this may happened owing to the breakdown of carbon skeleton present in MWCNTs (**Figure 4** (i)) [43]. Subsequently, we have also determined the weight loss in the process of formation of various functional groups like –COOH and -OH on the MWCNT. According to Figure 4 (ii)), we identified as 13% weight loss of MWCNT was owed to the sluggish reduction in oxidation functionalities at above 100 °C and this obtained results were corresponding to reported decomposition pattern in literature [44].

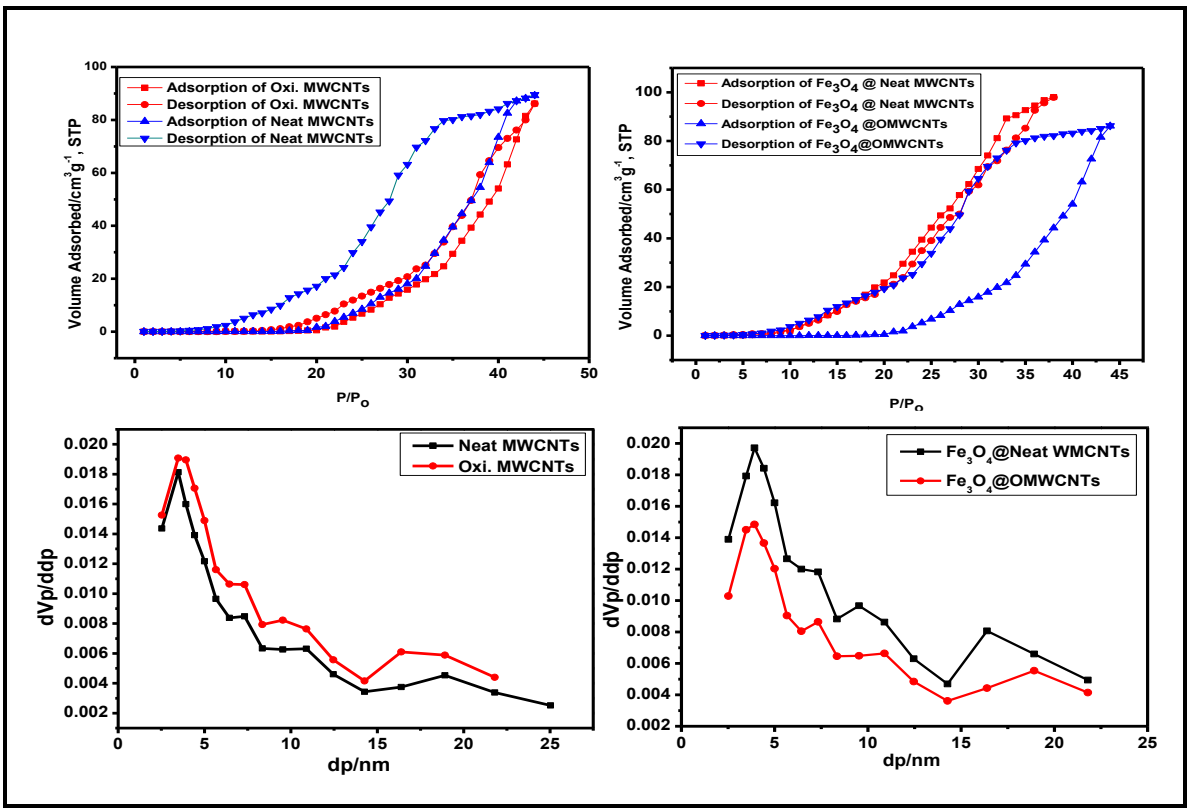

Sr. No.	Nano-Composite	Surface area (in m^2/g)	Pore size (in nm)	Pore Volume (in cm^{-1}/g)
1	Pure CNT's	117.48	3.93	0.1931
2	Oxidized CNT's	113.48	3.47	0.1761
3	Fe_3O_4@Oxidized CNT's	86.814	3.56	0.1423
4	Fe_3O_4@Neat CNT's	98.636	3.47	0.1516

Figure 3. Nitrogen adsorption-desorption curve and pore volume analysis using BET technique of (i) MWCNTs, (ii) OMWCNTs, and (iii) Fe_3O_4@OMWCNTs

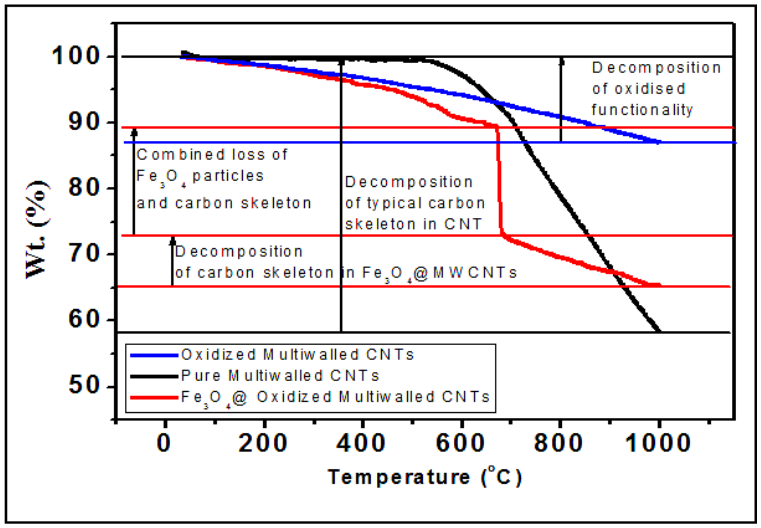

Figure 4. TGA analysis of (i) MWCNTs, (ii) OMWCNTs, and (iii) Fe_3O_4@OMWCNTs

Similar to OMWCNT, the prepared Fe_3O_4@OMWCNTs nano-composite showed near about 14% weight loss, which indicates the decomposition of oxidized functionality with rising the temperature from 100 °C to 590 °C. Furthermore, TGA graph of Fe_3O_4@OMWCNTs displayed huge weight loss within range of 670 °C to 690 °C, this indicated the breakdown of carbon skeleton and decomposition of Fe_2O_3 nanoparticles adhere on the surface of MWCNT [45]. Whereas, comprehensive weight loss pattern was observed at higher temperature range from 700 °C to 1000 °C, these results were parallel to the TGA pattern of OMWCNTs.

FE-SEM analysis of prepared heterogeneous catalyst

Figure 5 exhibited the morphology of neat MWCNT, OMWCNT, Fe_3O_4@OMWCNT, and Fe_3O_4 on neat MWCNT, investigated using SEM analysis. SEM images of MWCNTs displayed uniform surface whereas from the surface morphology of OMWCNT notable modification of surface was clearly observed through the introduction of acid functionality. Furthermore, grafting of Fe_3O_4 nano-particles on the OMWCNTs surface was performed by chemical method. The SEM images showed successful and uniform grafting of Fe_3O_4 nano-composite over the OMWCNTs surface. We trust that, the Fe_3O_4 nanoparticles are uniformly detached over OMWCNTs and that may owed to the hydrogen bonding between Fe and -COOH functionality [33, 41]. To know actual mechanism, one more experiments were conducted using non-oxidised MWCNT with same reaction parameter. Obtained results of SEM analysis reveals that, unequal and inferior amount of Fe_3O_4 nanoparticles were grafted over the surface of neat MWCNTs, this indicates lower interaction between Fe and MWCNTs due the absence of hydrogen bonding. Based on the results, we concluded as the oxidation of MWCNTs is a key process that fascinated the attraction forces among Fe and -COOH functionalities on MWCNTs, which facile to uniform distribution of Fe_3O_4 nanoparticles over wall of CNTs.

Furthermore, the crystal size of Fe_3O_4 nano-composite was observed same as 30-40 nm in both cases of OMWCNT and pure MWCNTs surface modification, which indicated successful growth of Fe_3O_4 nanoparticles on pure MWCNTs and OMWCNTs.

Elemental analysis (EDX) of prepared catalyst

Figure 6 showed the elemental composition of OMWCNT and Fe_3O_4@OMWCNT over and done with EDX analysis. The higher percentage of oxygen along with carbon indicated the successful formation of -COOH functional groups over the walls of CNTs.

Moreover, the EDX of Fe_3O_4-OMWCNT showed presence of C, Fe and especially with increased intensity of oxygen element, which assured that, grafting of Fe_3O_4 nano-particles on surface of OMWCNTs. In addition, from EDX analysis we can say that the formation of pure Fe_3O_4 nanoparticles and uniformly dispersed over the OMWCNTs without fabrication of impurities.

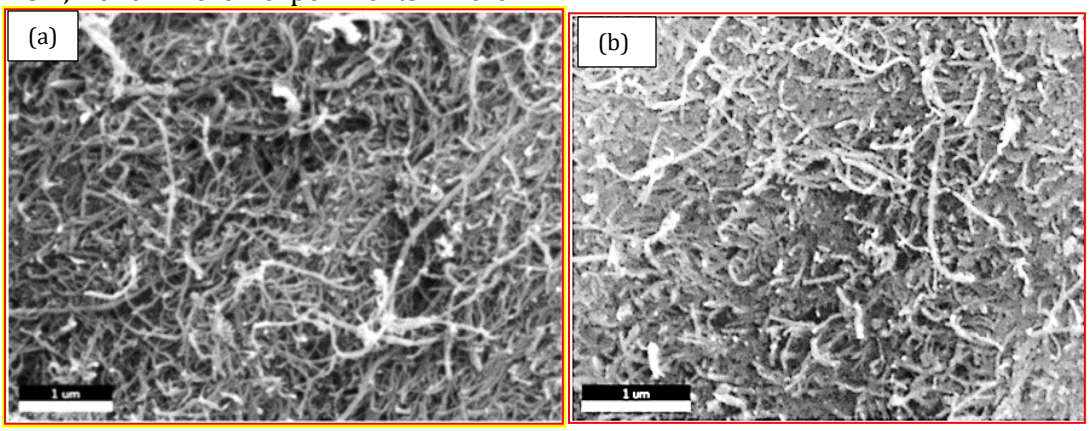

Figure 5. (a) SEM ofOMWCNTs and (b) SEM of Fe_3O_4@OMWCNT catalyst

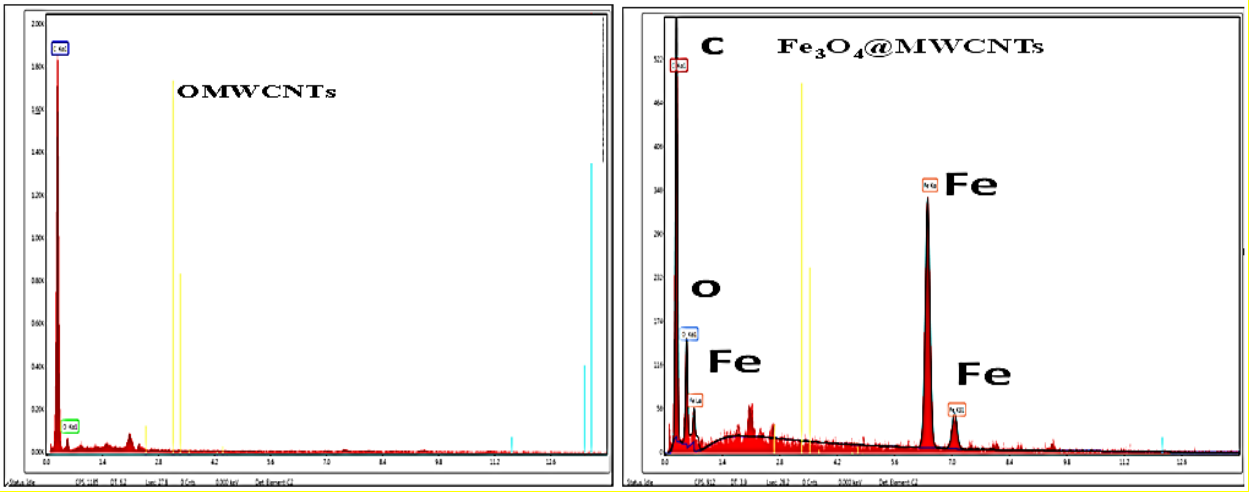

Figure 6. EDX mapping of OMWCNTs and prepared Fe_3O_4@OMWCNT catalyst

Catalytic Activity

Efficiency of OMWCNT-Fe_3O_4as heterogeneous catalyst for conversion of dimedone and substituted benzaldehyde to 1,8-dioxooctahydroxanthenes have been studied. The reaction condition was optimized through the model reaction as 2 mmol. dimedone and 1 mmol. benzaldehyde refluxed in 10 ml of solvent and their outcomes were summarized in **Table 1**. The initial attempt was carried out in catalyst free and solvent free atmosphere to check the reactivity of component; this displayed null conversion even to 42 hours stirring. Further reaction was performed at 100 ^{o}C under similar conditions as above, to determine effect of temperature on reaction; no isolated product was obtained (**Table 1**, entry 2). Next experiment was carried out in 10 ml ethanol as solvent without catalyst at reflux temperature for 24 hours; it reported fair 50 % yield (**Table 1**, entry 3).

Table 1. Influence of reaction parameters on the synthesis of 1,8-dioxooctahydro-xanthenes using Fe_3O_4@OMWCNT

Entry	Catalyst	Catalyst loading	Solvent	Temp. (^{o}C)	Time (h)	Yield (%)
1	-	-	-	RT	48	0
2	-	-	-	100	24	<10
3	-	-	Ethanol	Reflux	24	50
4	Fe_3O_4@OMWCNTs	10 wt %	-	RT	10	65
5	Fe_3O_4@OMWCNTs	10 wt %	Ethanol	Reflux	2	94
6	Fe_3O_4@OMWCNTs	10 wt %	Acetonitrile	Reflux	5	70
7	Fe_3O_4@OMWCNTs	10 wt %	Toulene	Reflux	5	65
8	Fe_3O_4@OMWCNTs	10 wt %	THF	Reflux	2	72
9	Fe_3O_4@OMWCNTs	7.5 wt %	Ethanol	Reflux	4	86
10	Fe_3O_4@OMWCNTs	5 wt %	Ethanol	Reflux	5	80
11	Fe_3O_4@OMWCNTs	15 wt %	Ethanol	Reflux	2	94
12	Fe_3O_4@OMWCNTs	20 wt %	Ethanol	Reflux	2	95

Next, the reaction was carried out in presence of wt % Fe_3O_4@OMWCNTs under solvent free and reflux condition to know the efficiency of catalyst; product was obtained with moderate 65 % yield after 10 h (**Table 1**, entry 4). The obtained results showed that the catalyst under solvent free atmosphere unable to produce efficient yield, so the same reaction was continued in 10 ml ethanol at reflux temperature. This exercise produced outstanding 94 % yield of xanthenes and major attraction of this experiment was shorter reaction time (**Table1**, entry 5). It was very necessary to check the productivity of various solvents compared to ethanol for current transformation and in presence of 10 wt % Fe_3O_4@OMWCNTs catalyst. To understand the influence of solvent on outputs of reaction, the number of solvents was screened for xanthenes production. The model reaction was tried in presence of Fe_3O_4@OMWCNTs in acetonitrile at reflux temperature gives moderate 70 % yield after 5 h (**Table 1**, entry 6). While the same reaction becomes slower in toluene solvent, resulted 65% yield in 5 h (**Table 1**, entry 7). Furthermore, next reaction was conducted in 10 ml THF solvent, it resulted 72% yield and it required only 2 h (**Table 1**, entry 8). This result showed respectable outcomes, but failed to overcome result of ethanol solvent. Screening test of solvent reveals, reaction performed in nonpolar solvent gave lower yield, while in polar solvent enhanced performance of reaction. Finally, ethanol was found to be better solvent for conversion of dimedone and bezaldehyde into 1,8-dioxooctahydroxanthene upto 94% yield. Subsequently, to set the optimised reaction parameters, we have tested different amount of prepared catalyst under reflux temperature in ethanol. Initially, we tried same reaction with reduction of catalytic amount with 7.5 wt. % and 5 wt. %; the reaction becomes sluggish with quite low yield 86 % and 80%, respectively (**Table 1**, entries 9 and 10). However, on increasing catalytic amount to 15 wt. % and 20 wt. %, both catalytic amounts are capable to produce equivalent yield as for 10 wt. % catalytic amount. Based on the atom economy and concern with principles of green chemistry; we finalized 10 wt. % catalytic amount for further investigations. Consequently, 10 wt. % catalytic amount and 10 ml ethanol under reflux condition was selected as optimized condition for the current transformation.

To understand catalytic efficiency of prepared catalyst, we have compared it with some other reported and available catalysts for the xanthene synthesis under described conditions, the obtained results were summarised in table 2. Synthesis of xanthenes using PTSA catalyst at high temperature 125 ^oC, the reaction was very sluggish gave 81-93% yield after 24 h (**Table 2**, entry 1). Further comparison with Fe^{3+}-Montmorillonite under reflux in ethanol for 6 h with 84-96% yield (**Table 2**, entry 2). Xanthene synthesis in presence of PPA-SiO_2 under reflux in acetonitrile, the reaction was found to be very slow and results into lower yield as 47% after 12 h (**Table 2**, entry 3). One more catalyst TMSCl, under reflux condition gave 72-84% yield within 8-10 h (**Table 2**, entry 4). After the comparison of these results compared with present methodology, it was clearly indicated that the Fe_3O_4@OMWCNT is highly efficient catalyst for conversion of dimedone to 1, 8-dioxooctahydroxanthene derivatives (**Table 2**, entry 5).

Table 2. Comparative study of various catalysts for the xanthene transformation

Entry	Catalyst	Condition	Time (h)	Yield (%) [Ref.]
1.	PTSA	125^oC	15-24	81-93 [25]
2.	Fe^{3+}-Montmorillonite	C_2H_5OH/reflux	6	84-96 [26]
3.	PPA-SiO_2	CH_3CN/reflux	12	47 [36]
4.	TMSCl	CH_3CN/reflux	8-10	72-84 [37]
5.	Fe_3O_4@OMWCNT	C_2H_5OH/reflux	2	90-96 [present work]

To examine the scope and applicability of present methodology, series of aromatic aldehydes were condensed with dimedone under optimized reaction condition. Monitoring of all reactions and their completion was confirmed by thin layer chromatography, time taken, and yield of product was summarized in **Table 3**. The dimedone and substituted aldehydes were undergoes cyclization in presence of little quantity of catalyst for short reaction time and furnished with moderated to outstanding yield. As it can be in **Table 3**, entry 1 is for the well set model reaction under optimised conditions, it clearly gives an idea about reactivity of aryl aldehyde with dimedone in presence of catalyst to give xanthenes. Entry 2 shows the result for para methyl substituted benzaldehyde, reaction ends with 90 % yield of targeted molecule which revealed that the decrease in reactivity due to presence of electron donating group on aryl aldehyde. Similar results were observed in case electron donating substituents on benzldehyde as 4-hydroxy and 4-methoxy substituted benzaldehydes, displayed 93 % and 92 % yield, respectively (**Table 3**, entries 3 and 4).

In addition, we have checked reactivity of 4-Chlorobenzaldehyde, 4-hydroxy-3-methoxybenzaldehyde, and 4-Flurobenzaldehyde under the optimized conditions. All these substituted aldehydes reported acceptable yield of respective derivatives (**Table 3**, entries 5-7). Moreover, electron-withdrawing groups such as $-NO_2$, -Cl, accumulated benzaldehyde reacted smoothly with efficient yield of xanthenes (**Table 3**, entries 8-11). Among the all substituted benzaldehydes, p-nitrobenzaldehyde reacts faster with high yield (**Table 3**, entry 9). From these outcomes of such exercise, we concluded as the sketched protocol has been well fitted for various substituted aromatic aldehydes carrying different functionalities. All such functionalities were preserved throughout the reaction process and consists in final products under the 10 wt. % Fe_3O_4@OMWCNT catalysed optimized protocol.

Proposed Mechanism

On the basis of formation of product in presence of Fe_3O_4@OMWCNT, we have constructed probable mechanism for development of xanthenes is shown in **Scheme 2**. The proposed mechanism has been supported by the literature data [30]. Initially dimedone undergoes keto-enol tautomerism to

Table 3. Synthesis of 1,8-dioxooctahydro xanthene derivatives using Fe_3O_4@OMWCNT under optimized protocol

Entry	Aldehyde	Time (h)	Product code	Yield (%)
1	Benzaldehyde	2.00	**3a**	94
2	4-Methylbenzaldehyde	3.30	**3b**	90
3	4-Hydroxybenzaldehyde	4.00	**3c**	93
4	4-Methoxybenzaldehyde	3.30	**3d**	92
5	4-Chlorobenzaldehyde	3.00	**3e**	94
6	4-Hydroxy-3-Methoxybenzaldehyde	3.20	**3f**	92
7	4-Flurobenzaldehyde	2.00	**3g**	92
8	3-Nitrobenzaldehyde	3.00	**3h**	95
9	4-Nitrobenzaldehyde	1.40	**3i**	96
10	3-Chlorobenzaldehyde	4.30	**3j**	94
11	4-Formylbenzaldehyde	4.00	**3k**	94

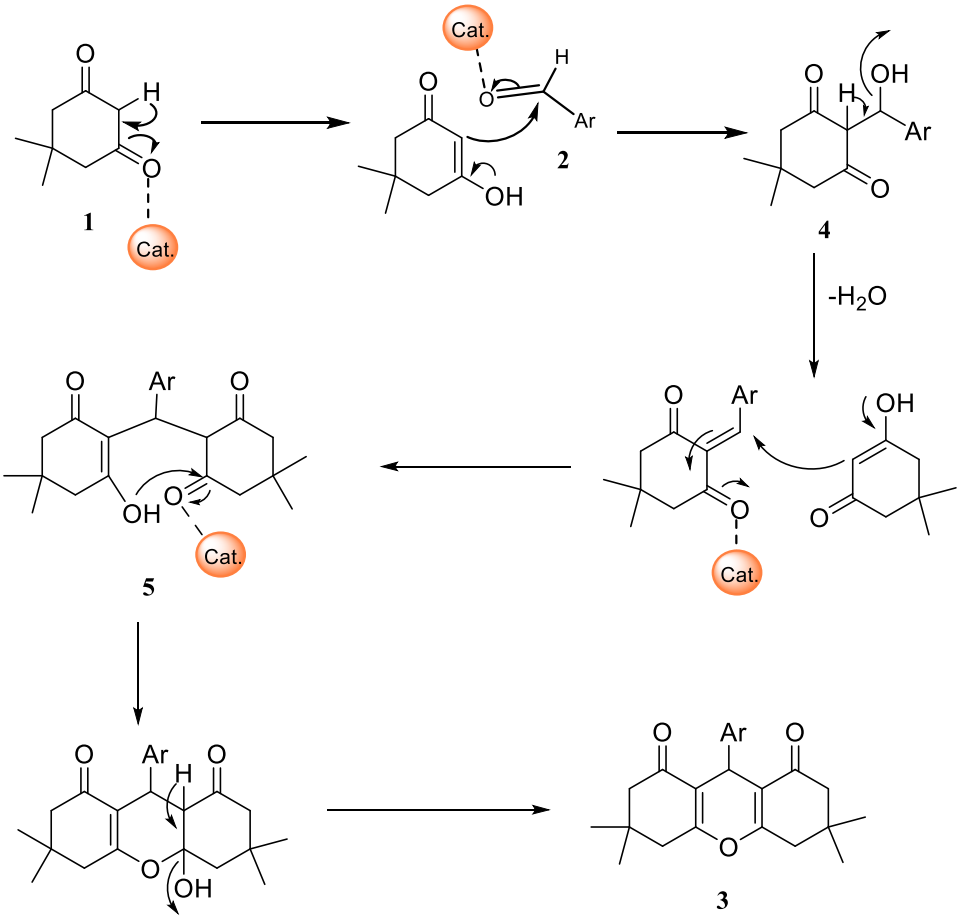

Scheme 2. Proposed mechanism for synthesis of xanthenes derivatives using Fe_3O_4@OMWCNT

form enol which is activated by Fe_3O_4@OMWCNT catalyst, and then secondly catalyst interacts with oxygen of aldehyde which leads to generation of carbonium ion. It facilitates nucleophilic attack of previous enol to form carbon-carbon bond. Furthermore, it undergoes dehydration, which provides site for repetitive nucleophillic attack of another enol of dimedone. Finally, catalyst plays key role in cyclization to achieve target molecule (**3**).

Recyclability test of Fe_3O_4@OMWCNT

Development of eco-friendly and reusable catalytic system was the ultimate goal of present research work. We have used Fe_3O_4@OMWCNT as heterogeneous nano-catalyst for 1,8-dioxooctahydroxanthenes synthesis. After the complete transformation, the catalyst was isolated simply using strong external magnet. Separated catalyst was washed with water and ethanol for two to three times, and then dried at 90 °C for 10-12 h, and then it has ready to use for next cycle. We have studied recyclability of prepared catalyst for prescribed model reaction as 2 mmol. Dimedone and 1 mmol. benzaldehyde were refluxed in 10 ml of EtOH and presence of 10 wt. % Fe_3O_4@OMWCNT. Catalyst was reused up to six cycles under optimized condition. Experimental results revealed that 1, 8-dioxooctahydroxanthene yield was comparable with consistent up to six run of catalyst.

Conclusion

In conclusion, Fe_3O_4@OMWCNT was utilized as heterogeneous catalyst for the conversion of aryl aldehyde and dimedone to xanthene derivatives. The catalyst was prepared and characterized successfully with help of various spectroscopic techniques that showed

oxidation of MWCNT leads to -COOH functionality as well as anchoring of Fe_3O_4 on MWCNTs. The catalyst proved itself as extremely resourceful for 1,8-dioxooctahydroxanthene synthesis. The experimental procedure is an environmental being protocol as well as it reported outstanding yield within manageable reaction time. Moreover, catalyst showed its catalytic efficiency up to six cycles without noticeable diminution in yield of product. Significance of this methodology is simplicity of operation, easy work up, recyclable catalyst, good yields with maximum purification, and short reaction time. The key attraction of this methodology is the use of magnetically separable and proficient catalyst.

Orcids

Mantosh B. Swami
https://orcid.org/0000-0003-4786-6613
Ganpat R. Nagargoje
https://orcid.org/0009-0003-3796-8496
Sushil R. Mathapati
https://orcid.org/0000-0003-0534-3478
Abhay S. Bondge
https://orcid.org/0000-0002-6249-7185
Arvind H. Jadhav
https://orcid.org/0000-0002-9128-1981
Sharad P. Panchgalle
https://orcid.org/0000-0001-9706-7567
Vijaykumar S. More
https://orcid.org/0000-0002-6110-8774

Acknowledgements

The authors would like to thank the Principal, Mahtama Basweshwar Mahavidyalay, Latur and Dr. Sudhakar Patil, Maharashtra Udaygiri Mahavidyalay,Udgir, for providing research facilities. They are also grateful to Dr. Arvind Jadhav, CNMS Jain University Banglore, for their support.

References

[1]. I. Nakamura, Y. Yamamoto, *Chem. Rev.*, **2004,** *104*, 2127-2198. [Crossref], [Google Scholar], [Publisher]

[2]. J. Zhou *et. al.*, *Green Chem.*, **2017,** *19*, 3400-3407. [Crossref], [Google Scholar], [Publisher]

[3]. H.N. Hafez, M.I. Hegab, I.S. Ahmed-Farag, A.B.A. El-Gazzar, *Bioorg. Med.Chem.Lett*, **2008**, *18*, 4538-4543. [Crossref], [Google Scholar], [Publisher]

[4]. J. Araujo, C. Fernandes, M. Pinto, M.E. Titrain**,** *Molecules*, **2019,** *24*, 314. [Crossref], [Google Scholar], [Publisher]

[5]. B. Baghernejad, M. Fiuzat, *Appl. Chem. Res.*, **2021,** *15*, 46-54. [Crossref], [Google Scholar], [Publisher]

[6]. S-J. Tao, S-H. Guan, W. Wang, Z-Q. Lu, G-T. Chen, N. Sha, Q-X. Yue, X. Liu, D-A. Guo, *J. Nat. Prod.*, **2009,** *72*, 117-124. [Crossref], [Google Scholar], [Publisher]

[7]. N. Mulakyala, P.V.N.S. Murthy, D. Rambabu, M. Aeluri, R. Adepu, G. Krishna, C.M. Reddy, K. Prasad, M. Chaitanya, C.S. Kumar, M. Basaveswara, M. Pal, *Bioorganic Med. Chem. Lett.*, **2012**, *22*, 2186-2191. [Crossref], [Google Scholar], [Publisher]

[8]. M.V. Lembege, S. Moreau, S. Larrouture, D. Montaudon, J. Robert, A. Nuhrich, *Eur. J. Med. Chem.*, **2008,** *43*, 1336-1343. [Crossref], [Google Scholar], [Publisher]

[9]. M.S. Kumar, J. Singh, S.K. Manna, S. Maji, R. Konwar, G. Panda, *Bioorg. Med. Chem. Lett.*, **2018**, *28*, 778-782. [Crossref], [Google Scholar], [Publisher]

[10]. A.K. Bhattacharya, K.C. Rana, M. Mujahid, I. Sehar A.K. Saxena, *Bioorg. Med. Chem. Lett.*, **2009,** *19*, 5590-5593. [Crossref], [Google Scholar], [Publisher]

[11]. A-E. Hay, M-C. Aumond, S. Mallet, V. Dumontet, M. Litaudon, D. Rondeau, P. Richomme, *J. Nat. Prod.*, **2004,** *67*, 707-709. [Crossref], [Google Scholar], [Publisher]

[12]. F. Zelefack, D. Guilet, N. Fabre, C. Bayet, S. Chevalley, S. Ngouela, B.N. Lenta, A. Valentin, E. Tsamo, M-G.D-Franca, *J. Nat. Prod.*, **2009,** *72*, 954-957. [Crossref], [Google Scholar], [Publisher]

[13]. K. Chibale, M. Visser, D.V. Schalkwyk, A. Saravanamuthu, P.J. Smith, A. Fairlamb,

Tetrahedron, **2003,** *59*, 2289-2296. [Crossref], [Google Scholar], [Publisher]

[14]. J.F. Callan, A.P. de Silva, D.C. Magri, *Tetrahedron*, **2005**, *61*, 8551-8588. [Crossref], [Google Scholar], [Publisher]

[15]. R. Singla, K.B. Gupta, S. Upadhyay, M. Dhiman, V. Jaitak, *Bioorg. Med. Chem*. **2018**, *26*, 266-277. [Crossref], [Google Scholar], [Publisher]

[16]. C.G. Knight, T. Stephens, *Biochem. J.,* **1989**, *258*, 683-687. [Crossref], [Google Scholar], [Publisher]

[17]. S.A. Hilderbrand, R. Weissleder, *Tetrahedron Lett*., **2007**, *48*, 4383-4385. [Crossref], [Google Scholar], [Publisher]

[18]. G. S-Ruf, H-T Hieu, J-P. Poupelin, *Naturwiss.,* **1975**, *62*, 584-585. [Crossref], [Google Scholar], [Publisher]

[19]. J-Q. Wang, R.G. Harvey, *Tetrahedron*, **2002,** *58*, 5927-5931. [Crossref], [Google Scholar], [Publisher]

[20]. A. Jha, J. Beal, *Tetrahedron Lett*., **2004**, *45*, 8999-9001. [Crossref], [Google Scholar], [Publisher]

[21]. D.W. Knight, P.B. Little, *J. Chem. Soc., Perkin Trans. 1,* **2001**, *4*, 1771-1777. [Crossref], [Google Scholar], [Publisher]

[22]. G. Casiraghi, G. Casnati, M. Comia, *Tetrahedron Lett*., **1973**, *14*, 679-682. [Crossref], [Google Scholar], [Publisher]

[23]. K. Dai, T. Peng, D. Ke, B. Wei, *Nanotechnology*, **2009**, *20*, 125603. [Crossref], [Google Scholar], [Publisher]

[24]. J. Li, S. Tang, L. Lu, H. C. Zeng, *J. American Chem. Soc*., **2007**, *129*, 9401-9409. [Crossref], [Google Scholar], [Publisher]

[25]. R. Lv, S. Tsuge, X. Gui, K. Takai, F. Kang, T. Enoki, J. Wei, J. Gu, K. Wang, D. Wu, *Carbon*, **2009,** *47*, 1141-1145. [Crossref], [Google Scholar], [Publisher]

[26]. L. Jiang, L. Gao, *Chem. Mater*., **2003**, *15*, 2848-2853. [Crossref], [Google Scholar], [Publisher]

[27]. Q. Li, Z. Chen, W. Ren, B. Liu, F. Li, H. Cong, H.M. Cheng, *Carbon*, **2008**, *46*, 1892-1902. [Crossref], [Google Scholar], [Publisher]

[28]. J. Wan, W. Cai, J.T. Feng, X. Meng, E. Liu, *J. Mater. Chem*., **2007**, *17*, 1188-1192. [Crossref], [Google Scholar], [Publisher]

[29]. J. Jang, H. Yoon, *Adv. Mater*., **2003**, *15***,** 2088-2091. [Crossref], [Google Scholar], [Publisher]

[30]. B. Karami, S.J. Hoseini, K. Eskandari, A. Ghasemi, H. Nasrabadi*, Catal. Sci. Technol*., **2012**, *2*, 331-338. [Crossref], [Google Scholar], [Publisher]

[31]. S. Kantevari, R. Bantu, L. Nagarapu, *J. Mol. Catal. A: Chem*., **2007**, *269*, 53–57. [Crossref], [Google Scholar], [Publisher]

[32]. K. Venkatesan, S.S. Pujari, R.J. Lahoti, K.V. Srinivasan, *Ultrason. Sonochem*., **2008**, *15*, 548–553. [Crossref], [Google Scholar], [Publisher]

[33]. A.K. Mishra, S. Ramaprabhu, *J. Phys.Chem. C,* **2010**, *114*, 2583–2590. [Crossref], [Google Scholar], [Publisher]

[34]. J. Zhang, H. Zou, Q. Qing, Y. Yang, Q. Li, Z. Liu, X. Guo, Z. Du, *J. Phys. Chem. B*, **2003**, *107*, 3712–3718. [Crossref], [Google Scholar], [Publisher]

[35]. F. Avilés, J.V. Cauich-Rodríguez, L. Moo-Tah, A. May-Pat, R. Vargas-Coronado, *Carbon,* **2009,** *47*, 2970-2975. [Crossref], [Google Scholar], [Publisher]

[36]. M. Theodore, M. Hosur, J. Thomas, S. Jeelani, *Mater. Sci. Eng. A,* **2011,** *528*, 1192–1200. [Crossref], [Google Scholar], [Publisher]

[37]. B. Wang, X. Zhou, Y. Wu, Z. Chen, C. He, *Sens. Actuators B Chem*. **2012,** *171-172*, 398–404. [Crossref], [Google Scholar], [Publisher]

[38]. G. Zhao, J.J. Feng, Q.L. Zhang, S.P. Li, H.Y. Chen, *Chem. Mater*. **2005,** *17*, 3154–3159. [Crossref], [Google Scholar], [Publisher]

[39]. N. Yan, X. Zhou, Y. Li, F. Wang, H. Zhong, H. Wang, Q. Chen, *Sci. Rep*. **2013**, *3*, 3392. [Crossref], [Google Scholar], [Publisher]

[40]. J. Thewlis, *J. Philos. Mag*. **1931**, *12*, 1089–1106. [Crossref], [Google Scholar], [Publisher]

[41]. D. Prasad, K.N. Patil, N. Sandhya, C.R. Chaitra, J.T. Bhanushali, A.K. Samal, R.S. Keri, A.H. Jadhav, B.M. Nagaraja, *Appl. Surf. Sci.*, **2019**, *489*, 538–551. [Crossref], [Google Scholar], [Publisher]

[42]. B.I. Kharisov, O.V. Kharissova, U.O. Mendez, I.F. Gomez, *Synth. React. Inorg. Met.,* **2015**, *46*, 55-76. [Crossref], [Google Scholar], [Publisher]

[43]. J.P.C. Trigueiro, G.G. Silva, R.L. Lavall, C.A. Furtado, S. Oliveira, A.S. Ferlauto, R.G. Lacerda, L.O. Ladeira, J.W. Liu, R.L. Frost, G.A. George, *J. Nanosci. Nanotechnol.*, **2007,** *7*, 3477–3486. [Crossref], [Google Scholar], [Publisher]

[44]. W.M. Silva, H. Ribeiro, L.M. Seara, H.D.R. Calado, A.S. Ferlauto, R.M. Paniago, C.F. Leitec, G.G. Silva, *J. Braz. Chem. Soc.*, **2012,** *23*, 1078-1086. [Crossref], [Google Scholar], [Publisher]

[45]. D. Yang, S. Xu, S. Dong, J. Liu, A. Guo, X. Yan, F. Hou, *RSC Adv.*, **2015**, *5*, 106298–106306. [Crossref], [Google Scholar], [Publisher]